The instability of a shear layer between two parallel streams

By ROBIN E. ESCH
Pierce Hall, Harvard University

(*Received* 10 *July* 1957)

SUMMARY

An unbounded parallel flow, consisting of a linear shear layer between uniform streams, is investigated for stability. A conventional eigenvalue problem is formulated, and solved by both analytical and numerical methods. The region of instability in the plane of Reynolds number R and disturbance wave number α is determined, and typical growth rates in the unstable region are computed.

Unstable disturbances are found at all values of R. Results for $\alpha R > 100$ are found to agree closely with inviscid theory results. An analytic method useful for $\alpha R < 1$ is developed.

The extent to which the present results can be applied to the laminar boundary layer between free streams is discussed.

1. INTRODUCTION AND PREVIOUS RESULTS

The stability of parallel flows has been studied extensively; an account of such work, as well as a discussion of the general significance of the hydrodynamic stability problem, has been given by Lin (1955). Most of the work to date has dealt with flows confined by one or more solid boundaries. Since instability occurs only at high Reynolds numbers for such flows, most of this work has made use of mathematical methods appropriate to high values of the Reynolds number. The present investigation, however, deals with an unbounded flow, at both high and low Reynolds numbers, and novel methods are introduced to treat the problem.

The flow that will be treated consists of two uniform streams of fluid moving parallel to one another, separated by a laminar shear layer. Such a model is relevant to the investigation of the boundary layer separating a water current from adjacent still water. It is also useful in predicting what happens when a shock wave diffracts into the shadow zone behind an obstacle; for a brief time after the passage of the shock wave, the velocity field will be approximately parallel, and of the form considered here. Information of interest in such problems is the characteristic size of the disturbances which may be expected to appear, and the rate at which they grow. The transient character of such flows (the shear layer, of course, grows in width) is ignored in the models considered here. Only infinitesimal disturbances are considered.

Probably the first unbounded flow stability analyses were by Helmholtz (Lamb 1945)—hence the name 'Helmholtz instability'—and Rayleigh (1945). Helmholtz considered inviscid fluids with a discontinuous profile, shown as profile (*a*) of figure 1; the two streams are thus considered to be separated by a vortex sheet of zero thickness. An infinitesimal disturbance with wave number α was found to grow at the rate $e^{\alpha c_i t}$ where t is time, and c_i is a constant. This growth factor αc_i is graphed

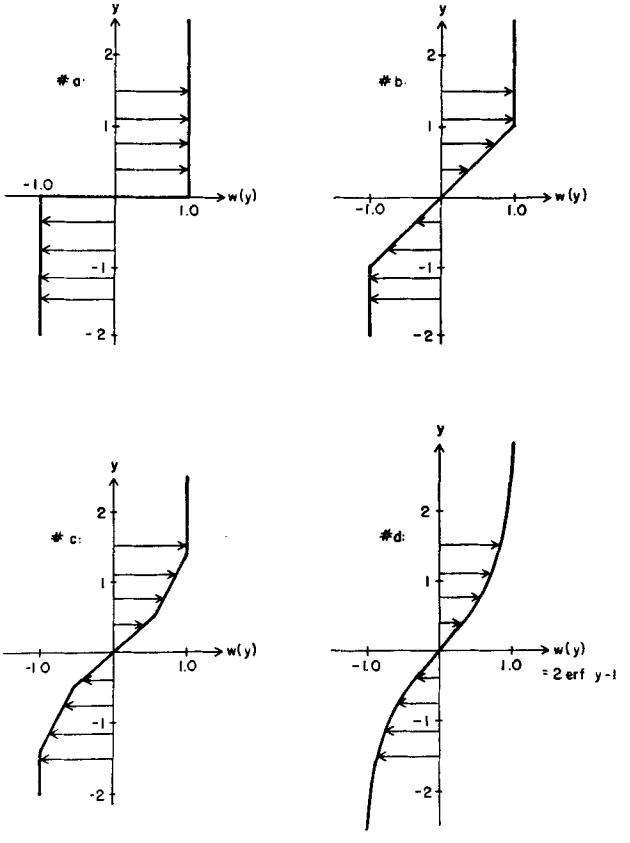

Figure 1. Velocity profiles.

in figure 2. Rayleigh, also assuming a perfect fluid, considered the piecewise linear profile (*b*) of figure 1. Such a profile is closer to the smooth profile to be expected in a real laminar boundary layer between two streams (similar to profile (*d*) in figure 1). The exponential growth factor found by Rayleigh is depicted in figure 2.

Carrier (1954), still considering zero viscosity, obtained an analytic solution for the piecewise linear profile (*c*) of figure 1, which is a closer approximation to profile (*d*). He also obtained a numerical solution for profile (*d*) itself. The results are shown in figure 2.

The first attempt to include viscosity in the analysis was made by Lessen (1950), who solved the boundary layer equations numerically to obtain a profile similar to (*d*) of figure 1. He obtained numerically the first two terms of an asymptotic approximation to the solution of the stability problem, thereby computing values of the disturbance growth factor for a certain region in the plane of Reynolds number R and disturbance wave number α. Lessen's results show that for such unbounded flows the physically interesting effects of viscosity occur at much lower Reynolds numbers than for flows confined by solid boundaries. Further, Lessen demonstrated that the slope of the neutral stability curve in the α, R plane is positive for very large R.

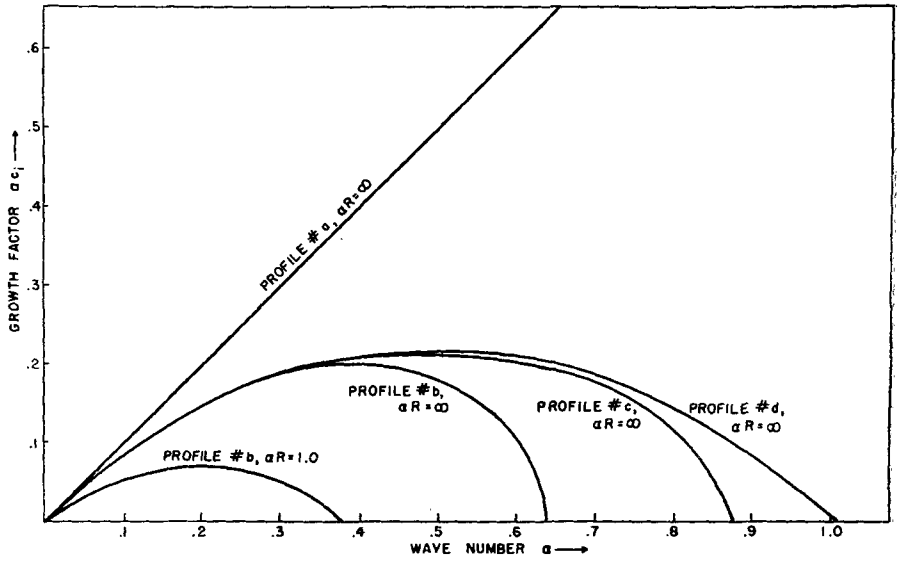

Figure 2. Growth factors. The corresponding profiles are shown in figure 1.

The present investigation treats the piecewise linear profile (*b*) of figure 1, extending the analysis to include the effects of viscosity. Although the resulting problem is only an approximate model for the physical problems stated earlier, the mathematical simplifications that result from this choice of profile allow exact solution of the eigenvalue problem at all values of Reynolds number. If the inviscid results may be taken as an indication, the present results will be quantitatively useful for profile (*d*) of figure 1 if the disturbance wave number α is small, but only qualitatively correct for larger values of α.

2. Mathematical formulation of the problem

The behaviour of small disturbances in the parallel flow of an incompressible fluid (cf. Lin 1955) are governed by the Orr–Sommerfeld equation

$$[w(y)-c](f''-\alpha^2 f)-w''(y)f = \frac{1}{i\alpha R}(f^{iv}-2\alpha^2 f''+\alpha^4 f) \qquad (1)$$

where $w(y)$ is the normalized steady velocity distribution whose stability is to be investigated; y is distance across the stream measured in units equal to the half-width H of the shear layer; and f, α, c, are defined by noting that the stream function associated with the disturbance velocity field is given by

$$\psi(x, y, t) = f(y)\exp[i\alpha(x - ct)]. \tag{2}$$

The Reynolds number R is $(U_m H/\nu)$, where U_m is the normalizing velocity, and ν is the kinematic viscosity of the fluid. The exponential growth factor is ac_i, where $c_i = \mathscr{I}(c)$; thus the steady velocity field is stable with respect to the disturbance if it is found that $c_i < 0$, and unstable if $c_i > 0$.

In the present problem the steady flow to be examined is

$$w(y) = \begin{cases} 1, & 1 \leqslant y, \\ y, & -1 \leqslant y \leqslant 1, \\ -1, & y \leqslant -1, \end{cases} \tag{3}$$

which is shown as profile (*b*) of figure 1. Equation (1) then becomes

$$(y - c)(f'' - \alpha^2 f) = \frac{1}{i\alpha R}(f^{\mathrm{iv}} - 2\alpha^2 f'' + \alpha^4 f), \qquad -1 < y < 1, \tag{4}$$

$$(\pm 1 - c)(f'' - \alpha^2 f) = \frac{1}{i\alpha R}(f^{\mathrm{iv}} - 2\alpha^2 f'' + \alpha^4 f), \qquad \begin{cases} y > 1, \\ y < -1. \end{cases} \tag{5}$$

It is to be noted that although the $w''f$ term of (1) does not appear in (4) and (5), its effect is not lost, but is merely concentrated on the sheets $y = 1$, $y = -1$. In fact, if the limits

$$\lim_{\varepsilon \to 0} \int_{-1-\varepsilon}^{-1+\varepsilon} \{\text{Equation (1)}\}\, dy \text{ and } \lim_{\varepsilon \to 0} \int_{1-\varepsilon}^{1+\varepsilon} \{\text{Equation (1)}\}\, dy$$

are considered, the $w''f$ term is found to lead to the requirement that

$$\left.\begin{aligned} \lim_{\varepsilon \to 0}[f'''(-1+\epsilon) - f'''(-1-\epsilon)] &= -i\alpha R f(-1), \\ \lim_{\varepsilon \to 0}[f'''(1+\epsilon) - f'''(1-\epsilon)] &= i\alpha R f(+1). \end{aligned}\right\} \tag{6}$$

The simple nature of equations (5) governing the *outer regions* $|y| > 1$ will allow the removal of these regions from the problem. The behaviour of the outer-region solutions, and the discontinuities in the derivative of $w(y)$, will then enter the problem in the form of boundary conditions on the centre-region equation (4). Equations (5) have the particular solutions

$$\left.\begin{aligned} f &= e^{\pm \alpha y}, \quad e^{\pm b_1 y}, \quad y > 1, \\ f &= e^{\pm \alpha y}, \quad e^{\pm b_2 y}, \quad y < -1, \end{aligned}\right\} \tag{7}$$

where $$b_1 = [\alpha^2 + i\alpha R(1 - c)]^{1/2}, \qquad b_2 = [\alpha^2 - i\alpha R(1 + c)]^{1/2}. \tag{8}$$

It will be assumed, and may be verified later, that $\mathscr{R}(b_1)$ and $\mathscr{R}(b_2)$ are never zero. Hence, with the appropriate choice of square root branches, b_1 and b_2 can be defined to have real parts greater than zero.

The general outer-region solutions will be linear combinations of the particular solutions (7). The boundary conditions at large $|y|$, which require that both components of disturbance velocity must decay, require the elimination of growing exponentials. Thus the outer-region solutions are

$$f = A_1 e^{-\alpha y} + A_2 e^{-b_1 y}, \qquad y > 1, \tag{9}$$

$$f = A_3 e^{\alpha y} + A_4 e^{b_2 y}, \qquad y < -1. \tag{10}$$

Returning to the equation governing $f(y)$ in the inner region $-1 < y < 1$, it is found that a general solution is

$$f = B_1 e^{\alpha y} + B_2 e^{-\alpha y} + B_3 f_3(y) + B_4 f_4(y), \tag{11}$$

where $e^{\alpha y}$, $e^{-\alpha y}$, $f_3(y)$ and $f_4(y)$ are four linearly independent solutions of (4). Applying the matching conditions, i.e. requiring f, f', and f'' continuous and f''' discontinuous as specified by (6), eight equations may be derived from (9) and (10). By eliminating the constants A_1, A_2, A_3, A_4 from these equations, the following four equations, which constitute boundary conditions on the inner-region solution (11), may be derived:

$$\left.\begin{aligned} f''(1) + (b_1 + \alpha) f'(1) + b_1 \alpha f(1) &= 0, \\ f'''(1) - (b_1^2 + b_1 \alpha + \alpha^2) f'(1) + (i\alpha R - b_1^2 \alpha - b_1 \alpha^2) f(1) &= 0, \\ f''(-1) - (b_2 + \alpha) f'(-1) + b_2 \alpha f(-1) &= 0, \\ f'''(-1) - (b_2^2 + b_2 \alpha + \alpha^2) f'(-1) + (i\alpha R + b_2^2 \alpha + b_2 \alpha^2) f(-1) &= 0. \end{aligned}\right\} \tag{12}$$

The centre-region equation, (4), plus these four boundary conditions, constitute a conventional eigenvalue problem, where $f(y)$ is the eigenfunction and c the eigenvalue. If equations (12), considered as equations in the unknown coefficients B_1, B_2, B_3, B_4, are to have non-trivial solutions, the determinant of the coefficients must vanish. Thus the secular equation (13) on p. 294 must be obeyed.

It remains to find acceptable representations for f_3 and f_4, the third and fourth solutions of (4), and to substitute them in (13), thereby obtaining a relationship among the parameters α, c and R. Solutions of (4) may be derived in the form of integrals of Bessel functions of order one-third, or integrals of Airy integrals (cf. Watson 1944, p. 188). However, representations of more immediate use may be obtained by taking the Fourier transform of equation (4). Defining

$$\phi(p) = \int_{-\infty}^{\infty} e^{-ipy} f(y)\, dy, \tag{14}$$

ϕ is found to obey the first-order equation

$$-i(p^2 + \alpha^2)\phi' + \left\{\frac{i}{\alpha R} p^4 + \left(c + \frac{2\alpha^2 i}{\alpha R}\right) p^2 - 2ip + \alpha^2 c + \frac{i\alpha^4}{\alpha R}\right\}\phi = 0, \tag{15}$$

which has the solution

$$\phi = 2\pi A \exp\left\{\frac{p^3}{3\alpha R} - i\left(c + \frac{i\alpha^4}{\alpha R}\right) p - \log[(p + i\alpha)(p - i\alpha)]\right\}. \tag{16}$$

$$\begin{vmatrix} 2\alpha(b_1+\alpha) & 0 & b_1\alpha f_3(1)+(b_1+\alpha)f_3'(1)+f_3''(1) & b_1\alpha f_4(1)+(b_1+\alpha)f_4'(1)+f_4''(1) \\ i\alpha R-2b_1^2\alpha-2b_1\alpha^2 & i\alpha Re^{-2\alpha} & (i\alpha R-b_1^2\alpha-b_1\alpha^2)f_3(1)- & (i\alpha R-b_1^2\alpha-b_1\alpha^2)f_4(1)- \\ & & -(b_1^2+b_1\alpha+\alpha^2)f_3'(1)+f_3'''(1) & -(b_1^2+b_1\alpha+\alpha^2)f_4'(1)+f_4'''(1) \\ 0 & 2\alpha(b_2+\alpha) & b_2\alpha f_3(-1)-(b_2+\alpha)f_3'(-1)+ & b_2\alpha f_4(-1)-(b_2+\alpha)f_4'(-1)+ \\ & & +f_3''(-1) & +f_4''(-1) \\ i\alpha Re^{-2\alpha} & i\alpha R+2b_2^2\alpha+2b_2\alpha^2 & (i\alpha R+b_2^2\alpha+b_2\alpha^2)f_3(-1)- & (i\alpha R+b_2^2\alpha+b_2\alpha^2)f_4(-1)- \\ & & -(b_2^2+b_2\alpha+\alpha^2)f_3'(-1)+f_3'''(-1) & -(b_2^2+b_2\alpha+\alpha^2)f_4'(-1)+f_4'''(-1) \end{vmatrix} = 0. \quad (13)$$

Consequently, defining for convenience

$$s = p(\alpha R)^{-1/3},$$

the desired function may be written

$$\left.\begin{aligned} f(y) &= \frac{1}{2\pi}\int e^{ipy}\phi(p)\,dp = AI, \\ I &= \frac{1}{(\alpha R)^{1/3}}\int \frac{\exp(i\Gamma s + \frac{1}{3}s^3)}{(s+i\Delta)(s-i\Delta)}\,ds, \\ \Gamma &= (\alpha R)^{1/3}[y - c - (i\alpha^2/\alpha R)], \\ \Delta &= \frac{\alpha}{(\alpha R)^{1/3}}, \end{aligned}\right\} \qquad (17)$$

where

and where the path of integration is either closed or approaches infinity in appropriate directions. That (17) is indeed a solution of (4) may easily be checked by direct substitution.

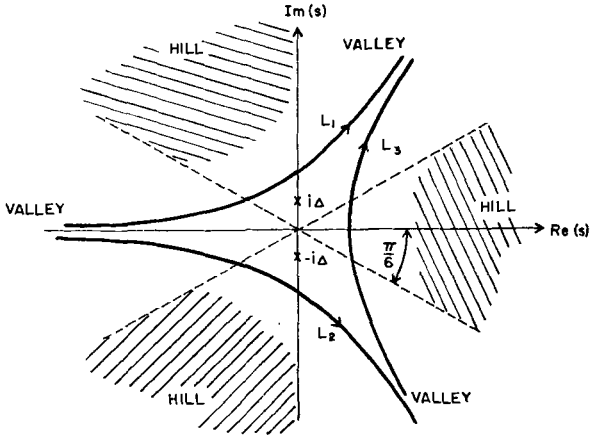

Figure 3. Paths in the s-plane.

Closed paths of integration about the simple poles at $s = i\Delta$ and $s = -i\Delta$ yield the two solutions $e^{\pm\alpha y}$, The remaining two independent solutions are obtained by considering paths with limits at infinity, such as L_1, L_2 or L_3 of figure 3. The corresponding integrals will be denoted I_1, I_2 and I_3. The paths must go to infinity in sectors in which the dominating factor of the integrand, $\exp(\frac{1}{3}s^3)$, is exponentially small. These sectors are the unshaded ones in figure 3.

3. Various methods of solution and results

Four methods, as enumerated below, were employed to obtain representations for f_3 and f_4 and thereby solve equation (13).

(*a*) *Large* αR. *Analytical method*

In most parallel flow stability investigations, the physically interesting phenomena have been found to occur at large Reynolds numbers (cf. Lin

1955). Consequently nearly all investigations to date have made use of asymptotic approximations valid for large Reynolds numbers. The first attack on the present problem made use of such a method.

Asymptotic approximations to the functions f_3 and f_4 were obtained from the integral representations (17) by the method of steepest descent integration (Watson 1944, p. 235ff). The following semi-convergent series in powers of $(\alpha R)^{-1/2}$ were thereby obtained:

$$I_1, I_2 = \begin{cases} I_b - I_a, \quad -I_a; & -\frac{3\pi}{2} < \arg\Gamma < -\frac{5\pi}{6}, \\ I_b, \quad\quad -I_a; & -\frac{5\pi}{6} < \arg\Gamma < -\frac{\pi}{6}, \\ I_b, \quad I_b - I_a; & -\frac{\pi}{6} < \arg\Gamma < \frac{\pi}{2}, \end{cases} \tag{18}$$

where

$$\left.\begin{matrix} I_a \\ I_b \end{matrix}\right\} \sim \frac{\pi^{1/2} \exp\{\frac{7}{8}\pi i \pm (\frac{1}{4}\pi i + \frac{2}{3} e^{i(\pi/4)}\Gamma^{3/2})\}}{(\alpha R)^{3/4}[y - c - (i\alpha^2/\alpha R)]^{1/4}(y-c)} \times$$

$$\times \left[1 + \frac{\pm (101/48) e^{-i(\pi/4)}}{(\alpha R)^{1/2}[y-c-(i\alpha^2/\alpha R)]^{3/2}} - \frac{(35905/4608)i}{\alpha R[y-c-(i\alpha^2/\alpha R)]^3} + O[(\alpha R)^{-3/2}]\right].$$

In the same manner, expressions were obtained for the first three derivatives of I_1 and I_2 (differentiating the asymptotic series (18) is not legitimate). Choosing $f_3(y) = I_1$, $f_4(y) = I_2$, the following asymptotic expansion of the secular equation (13) was derived:

$$KC_1 + KC_2(\alpha R)^{-1/2} + C_3(\alpha R)^{-1} + O[(\alpha R)^{-3/2}] = 0, \tag{19}$$

where

$$K = (1-2\alpha)^2 - 4\alpha^2\gamma^2 - e^{-4\alpha}, \qquad \gamma = c + \frac{i\alpha^2}{\alpha R},$$

$$C_1 = 4(1-\gamma^2),$$

$$C_2 = 2e^{i(\pi/4)}(1-\gamma)[2\alpha(1+\gamma)^{1/2} + (23/24)(1+\gamma)^{-1/2} +$$
$$+ 2e^{-i(\pi/4)}(1+\gamma)[2\alpha(1-\gamma)^{1/2} + (23/24)(1-\gamma)^{-1/2}],$$

$$C_3 = 16\alpha^2 i\gamma[4\alpha - 1 + 2\alpha^2 - 2\alpha^2\gamma^2] + K\Big\{2i(1-\gamma)\Big[\frac{71}{24}\alpha(1+\gamma)^{-1} +$$
$$+ \frac{4813}{2304}(1+\gamma)^{-2}\Big] - 2i(1+\gamma)\Big[\frac{71}{24}\alpha(1-\gamma)^{-1} + \frac{4813}{2304}(1-\gamma)^{-2}\Big] +$$
$$+ \Big[2\alpha(1-\gamma)^{1/2} + \frac{23}{24}(1-\gamma)^{-1/2}\Big]\Big[2\alpha(1+\gamma)^{1/2} + \frac{23}{24}(1+\gamma)^{-1/2}\Big]\Big\}.$$

Setting $(\alpha R)^{-1/2} = 0$, (19) reduces to $KC_1 = 0$, which yields

$$\alpha c = \pm \tfrac{1}{2} i[e^{-4\alpha} - (1-2\alpha)^2]^{1/2} \tag{20}$$

which is the result of Rayleigh (1945) for the inviscid case and is shown in figure 2.

Equating the sum of the first two terms of (19) to zero yields nothing more than the inviscid solution (20). It is therefore evident that the curves c = constant have a dependence on $(\alpha R)^{-1}$ that is of higher order than one-half.

Three terms of the series (19) are therefore necessary to determine the effect of finite Reynolds number. Equating their sum to zero yields a relation between α, αR and c, which was used to plot c = constant curves in the α, αR plane. These curves are presented in figure 4.

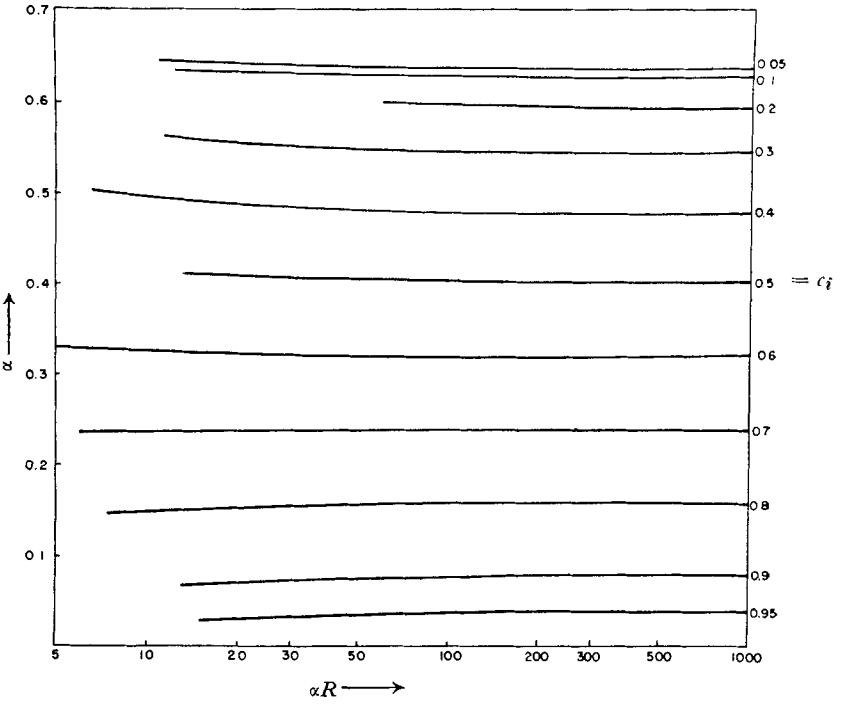

Figure 4. Asymptotic approximations to constant c lines.

From numerical investigations it was concluded that this asymptotic approach was accurate only for $\alpha R > 100$ (a comparison of the $c_i = 0{\cdot}4$ curve with numerical results is shown in figure 5; the values of the integrals (18) were also compared with values obtained by numerical integration). Thus, for $\alpha R > 100$, it may be concluded that there is almost no dependence of $\alpha(c_i, R)$ upon R.

It should be noted that the complex secular equation (13) constitutes in fact two relationships among the four parameters α, R, c_r and c_i. One of these relationships was always found to be satisfied by taking the phase velocity $c_r = 0$. Since the disturbance phase velocity arises from the convection of the disturbance by the steady flow (3), $c_r = 0$ corresponds to a disturbance centred at the midpoint of the shear layer (this interpretation loses its significance for small α, however, since the scale of the disturbance then becomes much larger than the shear layer width). This centring of the disturbance would be expected in the case of the real boundary layer, figure 1 (*d*), because of the point of inflection at the midpoint (cf. Lin 1955). Furthermore, it is found in the inviscid case

(equation (20)) that $c_r = 0$ for all wave numbers α in the unstable range. Though it has of course not been proven that disturbances with $c_r \neq 0$ do not exist, no such roots of the secular equation (13) could be found, even when c_r was deliberately made non-zero in the numerical investigations to be reported below.

A similar set of $c =$ constant curves was obtained for negative values of c_i, i.e. decaying disturbances. For the $c_i = 0$ (neutral stability) case, dependence on αR became of higher order; the only conclusion drawn was that

$$\left[\frac{d\alpha}{d(\alpha R)^{-1}}\right]_{c_i = 0,\,(\alpha R)^{-1} = 0} = 0. \tag{21}$$

(*b*) *Large αR. Numerical method*

In order to determine the region for which the asymptotic approximation is accurate, to extend the solution of the eigenvalue problem to lower values of αR, and to trace the neutral stability curve, a numerical method for large αR was sought. At large αR an error-control problem arises, due to the rapid oscillation both of $f(y)$ and of its Fourier transform. It was decided to integrate the integral representations (17) numerically along the steepest descent paths in the complex s plane. The advantages of this method are: (1) No oscillation of the integrand takes place, since the imaginary part of the exponent is by definition constant on such a path; the error problem caused by such oscillation, which increases in severity as αR increases, is thereby avoided. (2) The modulus of the integrand decreases most rapidly along such a path, allowing earliest termination of the integration. Indeed, because of these two features, the method works best for large αR, the very case for which other methods break down. The disadvantages of the method are: (1) the method is laborious; not only must the integrand be evaluated at each step but so must the quadrature formula coefficients and the integration contour location. (2) The necessity of dealing with complex numbers is expensive in computer time and internal storage space. (3) Auxiliary investigations must be made to find in what direction the steepest descent paths go to infinity, on what sides they pass the poles, and whether they pass too close to a pole.

The following complex generalization of the familiar Simpson's rule was found useful to extend the integration in the complex plane:

$$\left.\begin{aligned}
&\int_{z_0}^{z_2} g(z)\,dz = C_1\,g(z_0) + C_2\,g(z_1) + C_3\,g(z_2) + T,\\
&\text{where}\qquad C_1 = \frac{3\Delta_2\Delta_1^2 + 2\Delta_1^3 - \Delta_2^3}{6\Delta_1(\Delta_2 + \Delta_1)},\\
&\qquad\qquad C_3 = \frac{3\Delta_2^2\Delta_1 + 2\Delta_2^3 - \Delta_1^3}{6\Delta_2(\Delta_1 + \Delta_2)},\\
&\qquad\qquad C_2 = \Delta_2 + \Delta_1 - C_1 - C_3,\\
&\qquad\qquad \Delta_1 = z_1 - z_0, \qquad \Delta_2 = z_2 - z_1,\\
&\qquad\qquad |T| \leqslant (1/24)|g'''|_{\max}(|\Delta_1|^4 + |\Delta_2|^4).
\end{aligned}\right\} \tag{22}$$

The values of $f_3(\pm 1)$ and $f_4(\pm 1)$ found by this method were substituted into (13), and roots of (13) were found by successive approximation. The resulting points are shown on figure 5.

(*c*) *Small* αR. *Numerical method*

A numerical method which was economical for small αR was desired, in order to explore that region numerically, to aid in suggesting the proper approach that should be taken in a small αR analytic theory, and to allow the investigation of other profiles $w(y)$. Therefore a second numerical method, utilizing direct numerical solution of the differential equation (1), was programmed for machine solution.

The roots of the secular equation that were computed by this method are plotted in figures 2 and 5. At $\alpha R = 1$, the maximum growth rate was found to have decreased to less than one-half of its value at $\alpha R = \infty$. It was noted that, for small αR, a good empirical fit to the neutral stability curve is obtained by the curve

$$\alpha/(\alpha R)^{1/2} = \text{constant}, \tag{23}$$

the constant being near 0·4.

Finally, a small number of computations were done with the error-function profile, curve (*d*) of figure 1. The boundary conditions which must be taken for such a calculation require that the function and its first three derivatives, evaluated at $y = \pm A$ (where A is some sufficiently large number), must be continuous with the solutions (9) and (10) valid in the outer regions. The resulting boundary conditions are (12), with the $i\alpha R$ terms deleted, and where f is evaluated at $\pm A$ instead of ± 1.

Due to the lack of availability of machine time, only a single neutral stability point was computed for the error-function profile. It is plotted on figure 5, and is found to lie close to the neutral stability curve of the piecewise linear profile.

(*d*) *Small* αR. *Analytical method*

Since both α and R are small in the low Reynolds number instability region, the choice of a parameter in which to expand (13) is not obvious. The proper approach is indicated by the numerical results mentioned earlier, which suggest that

$$\alpha/(\alpha R)^{1/2} = \delta \tag{24}$$

tends to a non-zero constant as $\alpha R \to 0$ along the neutral stability curve. Consequently the secular equation (13) was re-written with α and R replaced by the parameters αR and δ, and an expansion of the form

$$\sum_{n=0}^{\infty} D_n(\alpha R)^{an} \tag{25}$$

was sought, where a is some simple fraction. The parameter c_i was set equal to zero, in order to obtain the neutral stability curve, and $c_r = 0$ was tried, on the basis of the numerical results reported above.

The differential equation (4), rewritten in terms of δ and αR, is

$$f^{iv} + \alpha R(-2\delta^2 - iy)f'' + (\alpha R)^2(\delta^4 + i\delta^2 y)f = 0. \tag{26}$$

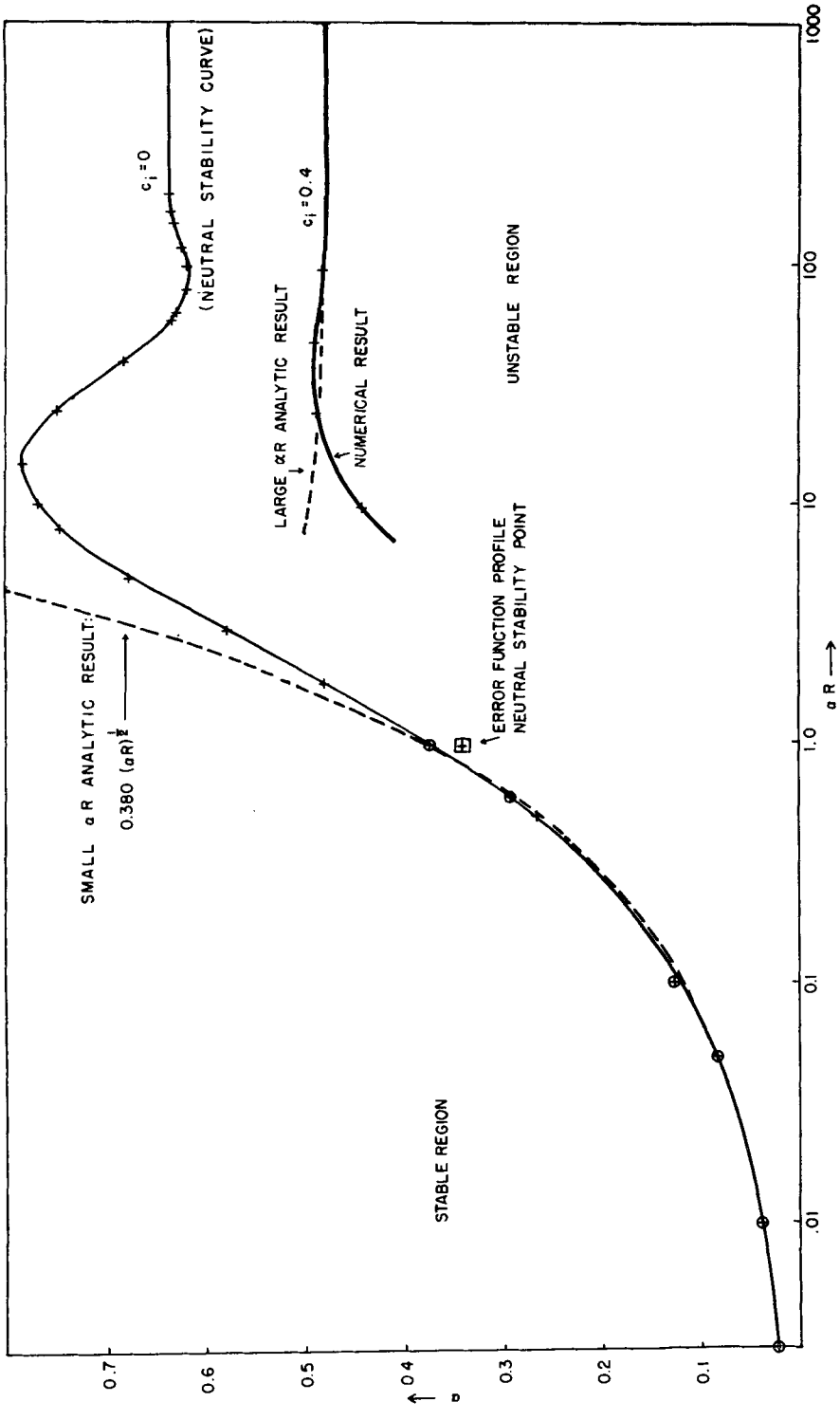

Figure 5. Results plotted in the $(\alpha, \alpha R)$ plane. Results of the numerical method for large αR are indicated by crosses, those for small αR by circled crosses.

Representations of solutions that converge rapidly for αR small at $y = \pm 1$ may be obtained by expanding f in a power series in the independent variable y (the practicability of this approach may be seen by substituting $z = (\alpha R)^{1/2}y$ into (26), and noting the analyticity of $f(z)$; for, as values of $f(y)$ are required at $p = \pm 1$, values of $f(z)$ are required only at the small points $z = \pm(\alpha R)^{1/2}$). In this manner the following particular solutions, linearly independent of the solutions $e^{\pm\alpha y} = e^{\pm\delta(\alpha R)^{1/2}y}$ already used, were obtained:

$$\left.\begin{aligned} f_3 &= 1 - \frac{\delta^4(\alpha R)^2}{24}y^4 - \frac{i\delta^2(\alpha R)^2}{120}y^5 - \frac{\delta^6(\alpha R)^3}{360}y^6 - \frac{i\delta^4(\alpha R)^3}{1008}y^7 + \dots, \\ f_4 &= y - \frac{\delta^4(\alpha R)^2}{120}y^5 - \frac{i\delta^2(\alpha R)^2}{360}y^6 - \frac{\delta^6(\alpha R)^3}{2520}y^7 + \dots. \end{aligned}\right\} \tag{27}$$

The resulting representation of the secular determinant (13) is a series in $(\alpha R)^{1/2}$. The first two terms of this series have coefficients that are identically zero; they may be removed and the algebra may be simplified by judicious manipulation of the rows and columns of the determinant. Equating to zero the first term that does not vanish identically yields the equation

$$2i\delta[\delta + (\delta^2 - i)^{1/2}][\delta + (\delta^2 + i)^{1/2}] + (\delta^2 - i)^{1/2} - (\delta^2 + i)^{1/2} = 0, \tag{28}$$

which for positive real δ has the single root

$$\delta = \frac{\alpha}{(\alpha R)^{1/2}} = 0{\cdot}380. \tag{29}$$

This then must be the asymptotic form of the neutral stability curve as $\alpha R \to 0$. Equation (29) is plotted in figure 5, and is seen to yield a good approximation to the neutral stability curve all the way up to the surprisingly large value $\alpha R = 1{\cdot}0$.

4. Conclusions and discussion

The inviscid theory result (figure 2) has been found to be a good approximation to the true situation for all $\alpha R > 100$. It would seem highly probable that this is not an accident associated with the particular profile investigated, but is true also of related profiles such as that of figure 1 (*d*). Though perhaps not of great theoretical interest, such a result might have considerable practical value.

From the results plotted on figure 5, it is seen that, as αR decreases to smaller values, the neutral stability curve first turns down to smaller wave numbers α. This is in agreement with the results of Lessen (1950) for the boundary layer between free streams. However, beginning at about $\alpha R = 100$, or $R = 170$, the curve turns upwards. A maximum is reached at about $\alpha R = 15$, $R = 20$, with $\alpha = 0{\cdot}78$, which is considerably higher than the asymptote $\alpha = 0{\cdot}64$ at $\alpha R = \infty$. The curve then descends to small values of α as αR is reduced further. Such behaviour is not found in Lessen's results, which are based on asymptotic approximations valid at large αR,

and, of course, on a different steady velocity profile. As shown in figure 5, the present asymptotic theory also fails to predict such behaviour. Consequently there is reason to suspect that the qualitative discrepancy between Lessen's results and the present results is due to inadequacy of asymptotic approximations, rather than to difference in profile. The present asymptotic expansions, which are power series in $(\alpha R)^{-1/2}$, are accurate only for $(\alpha R)^{1/2} > 10$, i.e. $\alpha R > 100$, even though they were carried out to three terms. It might therefore be suspected that the asymptotic approximation techniques conventionally used in parallel flow stability investigations are likely not to be profitable in unbounded shear-flow problems.

It is also fruitful to compare the present results with the results of the analysis of Lin (1955) for the stability of the flat plate boundary layer. The flat plate boundary layer results differ from the present results in that the region of instability in the α, αR plane is smaller, does not extend down to $\alpha = 0$ except at infinite Reynolds number, and does not extend below a minimum 'critical' Reynolds number; however, a relative maximum of the neutral stability curve is found in both cases. The presence of a solid boundary should certainly be expected to have a stabilizing effect; however, the following crude physical reasoning may perhaps further explain the differences. At a given Reynolds number, the amount of energy lost by viscous attenuation increases with wave number; therefore neither flat plate nor unbounded shear layer can be unstable at high α. Small α, on the other hand, corresponds to long wavelength (as seen from (2) the dimensional wavelength is $(2\pi H/\alpha)$, where H is the shear layer half-width). Suppose that a disturbance eigenmode dies out in the direction perpendicular to the shear layer in a distance of a wavelength (or in some distance simply related to the wavelength); then, in the flat-plate case, since the disturbance must be zero at the plate, at small α the main part of a disturbance would be situated entirely outside of the shear layer, a condition unfavourable for the excitation of the disturbance. However, in the absence of a solid boundary, the disturbance could straddle the shear layer in such a way that its excitation was optimized. This would explain the instability at small α, and absence of a positive critical Reynolds number in the present results.

The analytic method making use of ascending power series has been found to give accurate results for $\alpha R < 1$. It should also prove useful in computing growth rates within the unstable region for $\alpha R < 1$.

Although for the present problem there exists no positive critical Reynolds number, i.e. no $R > 0$ below which no instability exists, in practical cases such a critical R will result because an experiment is limited in size. The bounded geometry will imply a maximum disturbance wavelength, and hence a minimum $\alpha > 0$, and the critical R will occur when the neutral stability curve of figure 5 falls to that value of α.

Finally, it may be pertinent to estimate the extent to which the present results apply to related profiles such as figure 1(*d*). By the reasoning of Carrier (1954), it may be argued that agreement among results for related

profiles will be good for small α; for the width of the shear layer will then be small compared to a wavelength, and the motion of the disturbance, which will extend in the y direction effectively the order of a wavelength, will penetrate deeply into the uniform flow layers. In other words, if one wavelength is made the unit of distance, the shear layer becomes very thin, and all profiles on figure 1 look nearly the same. Judging from the inviscid results (figure 2), agreement should be good quantitatively for $\alpha < 0{\cdot}3$. The single neutral stability point calculated for profile (*d*) of figure 1 corroborates this assertion (see figure 5). For $\alpha > 0{\cdot}3$, however, agreement will be only qualitative, the internal structure of the shear layer becoming important.

Most of the work reported here was included in a doctoral thesis submitted in December, 1956, to Harvard University. The problem was suggested by Professor George Carrier, for whose continuing guidance the author is deeply grateful. The advice and help of Professor Sydney Goldstein, Professor Kenneth Iverson, and Mr Peter Neumann are gratefully acknowledged. The machine computations were made possible by the United States Air Force and by the cooperation and help of many members of the Harvard Computation Laboratory. The completion of the work was supported by the Office of Naval Research.

References

Carrier, G. 1954 Interface stability of the Helmholtz type, *Los Alamos Internal Report*.

Lamb, H. 1945 *Hydrodynamics*. New York : Dover.

Lessen, M. 1950 On stability of free laminar boundary layer between parallel streams, *Nat. Adv. Comm. Aero., Wash.*, no. 979.

Lin, C. C. 1955 *Theory of Hydrodynamic Stability*. Cambridge University Press.

Rayleigh, Lord 1945 *Theory of Sound*. New York : Dover.

Watson, G. N. 1944 *Theory of Bessel Functions*. Cambridge University Press.